

TAM Report No. 244

YIELD BEHAVIOR OF POLYCRYSTALLINE NIOBIUM

by
D. C. Huffaker
G. M. Sinclair

Department of Theoretical and Applied Mechanics
University of Illinois
Urbana, Illinois
May 1963

ABSTRACT

The yield behavior of niobium (columbium) has been studied under conditions of different states of stress, temperatures and strain rates, material compositions and microstructures.

Using data gathered in the present investigation as well as that obtained from ten other sources, it is shown that a relationship including the above variables is given by:

$$\dot{\gamma}_G = A e^{-\frac{[\Delta H^* - V (\tau_G - \tau_{iG})]}{RT}}$$

While details of the frequency factor A remain unclear, it appears that it may be treated as a constant over a wide range of temperatures and strain rates.

The analysis included in this paper shows that a simple parameter representation of yield behavior of niobium is feasible in terms of pertinent engineering variables.

ACKNOWLEDGEMENT

This investigation was conducted in the Department of Theoretical and Applied Mechanics of the University of Illinois. Financial support was made available by the United States Atomic Energy Commission under Contract AT(11-1)-1046. Acknowledgement is due Ralph Stewart for his assistance in the reduction of the data, Miss Kathryn Miller for the final preparation of the graphs, and Mrs. Hazel Corray who typed the manuscript.

TABLE OF CONTENTS

	Page
1.0 INTRODUCTION	1
1.1 Background	1
1.2 Object and Scope	2
2.0 MATERIAL, PREPARATION OF SPECIMENS, AND APPARATUS	3
2.1 Material	3
2.2 Preparation of Specimens	3
2.3 Apparatus	3
3.0 RESULTS	5
4.0 DISCUSSION AND ANALYSIS OF RESULTS	6
4.1 The Dependence of Yield Stress on State of Stress	6
4.2 The Dependence of the Yield Stress on Temperature and Strain Rate	8
4.3 The Dependence of the Yield Stress on Composition and Microstructure	9
5.0 SUMMARY AND CONCLUSIONS	11
6.0 REFERENCES	12
7.0 APPENDIX: Definition of Terms	14

LIST OF TABLES AND FIGURES

Table Number		Page
Ia.	Material Compositions for Investigation Included in this Report	15
Ib.	Grain Sizes and Heat Treatments	16
Ic.	Tabulated Yield Data	17
Figure Number		
1.	The Geometry of the Torsion Specimens	
2.	Effect of Strain Rate and Temperature on Upper Yield Point of Niobium. (present investigation)	
3.	Photomicrograph of Specimen Loaded at $\dot{\gamma} = 0.0001/\text{sec.}$, $T = 77^{\circ} \text{K}$	
4.	Frequency Factor, A , as Determined from Strain Rate and Temperature Dependence of Yield Point in Niobium (present investigation)	
5a.	Upper Yield Stress as a Function of Temperature and Strain Rate for Torsion Data (present investigation)	
5b.	Upper Yield Stress as a Function of Temperature and Strain Rate for Tensile Data (Wessell and Lawthers, 17)	
5c.	Upper Yield Stress as a Function of Temperature and Strain Rate for Tensile Data (Adams, Roberts and Smallman, 18)	
5d.	Upper Yield Stress as a Function of Temperature and Strain Rate for Tensile Data (Tankins and Maddin, 19)	
5e.	Upper Yield Stress as a Function of Temperature and Strain Rate for Tensile Data (Dyson, Jones and Tegart, 20)	
5f.	0.2% Offset Yield Stress as a Function of Temperature and Strain Rate for Tensile Data (Wilcox, Brisbane and Klinger, 21)	
5g.	0.2% Offset Yield Stress as a Function of Temperature and Strain Rate for Tensile Data (Mincher and Sheely, 22)	
5h.	0.2% Offset Yield Stress as a Function of Temperature and Strain Rate for Tensile Data (Begley and France, 23)	
5i.	Lower Yield Stress as a Function of Temperature and Strain Rate for Tensile Data (Churchman, 24)	
5j.	Proportional Limit Yield Stress as a Function of Temperature and Strain Rate for Tensile Data (A. A. Johnson, 25)	

List of Tables and Figures continued

Figure
Number

- 5k. 0.01% Offset and 0.05% Offset Yield Stress as a Function of Temperature and Strain Rate for Tensile and Compression Data, Respectively (Wessel, France and Begley, 26)
- 6. Dependence of Upper Yield Stress on Grain Diameter
- 7. Parameter Representation of the Temperature and Rate Sensitive Component of Yield Stress for Niobium

1.0 INTRODUCTION

1.1 Background

Earlier investigations have shown that an important factor of the ductile to brittle transition behavior in body centered cubic metals is the rapid increase in the yield stress within a relatively narrow range of temperatures. Briefly, it appears that a critical value of tensile stress is necessary to propagate a microcrack formed by the act of yielding. Any circumstance which raises the yield stress of the material above this critical stress establishes the condition for rapid fracture, i. e., brittle behavior. This rapid increase in the yield stress and its significance to the ductile to brittle transition phenomenon has been previously discussed and summarized in detail by Cottrell, Petch, Orowan, Bechtold and others ^{(1)*}.

Since the rapid rise in yield stress is an important factor in brittle fracture behavior, a simultaneous analysis of the variables affecting the yield stress is required so that the effects of each individual variable on the ductile to brittle transition phenomena can be properly evaluated. Among the more important variables related to engineering design are state of stress, temperature and strain rate, chemical composition and microstructure.

The state of stress determines the relative magnitudes of the principle stresses which in turn determine the value of the octahedral shear stress ⁽²⁾ a quantity used to predict macroscopic yielding in ductile materials ⁽³⁾.

The effect of temperature and strain rate on the yield behavior of iron and other body centered cubic metals seems to be characterized by a simple rate process equation ^(4, 5, 6, 7). This relationship describes many physical phenomena which are temperature and rate sensitive ^(8, 9). The general form of the equation is

$$\frac{1}{\dot{\epsilon}} = A e^{\frac{-\Delta H}{RT}} \quad (1)$$

In terms of the variables of interest in yield behavior, $\frac{1}{\dot{\epsilon}}$ may be considered as the strain rate (hereafter denoted by $\dot{\gamma}$). Present evidence relating to yielding and flow of BCC metals also suggests that ΔH is stress dependent ^(4, 5, 7, 10, 11, 12), that is

* Numbers in parentheses refer to list of references.

(using the notation given in the appendix)

$$\Delta H = \Delta H^* - V (\tau - \tau_i) \quad (2)$$

Thus, the modified form of the rate relation is

$$\dot{\gamma} = A e^{-\frac{[\Delta H^* - V(\tau - \tau_i)]}{RT}} \quad (3)$$

1.2. Object and Scope

The primary purpose of this investigation was to study the yielding of niobium, one of the BCC metals. Specifically, it was desired to study the influence of temperature and strain rate on the upper yield point of commercially pure niobium which had been further purified by heat treatment.

In this investigation, the temperature was varied from 77°K (the boiling point of liquid nitrogen) to 580° K. The three torsional strain rates utilized were 0.0001, 0.25, and 12.5/sec. These figures represent a temperature range of more than 500° K and a difference in strain rates of more than five orders of magnitude.

A secondary purpose of this study was to further explore the yield behavior of niobium by analyzing data from other investigations as well as that collected in this investigation. By utilizing data obtained from other sources in conjunction with the data collected in this investigation, a study of the effects of state of stress as well as composition and microstructure also become possible.

2.0 MATERIAL, PREPARATION OF SPECIMENS, AND APPARATUS

2.1. Material

The material used in this investigation was obtained from the Fansteel Metallurgical Corporation in the form of 9/16 in. diameter rod. The maximum amount of substitutional impurities in the as-received material is listed in Table I. The amounts of hydrogen, oxygen, nitrogen and carbon reported in Table I for this investigation were obtained by analysis after the metal had undergone heat treatment and will be discussed later in this paper.

2.2. Preparation of Specimens

The nominal dimensions of the torsion specimens are shown in Fig. 1. In addition to the specifications shown on the drawing, the outside surface of each specimen was polished and the inside surface was finished with a reamer. The critical dimensions were held constant within ± 0.003 in.

After the machining operations, the specimens were cleaned first in benzene, then in acetone, to remove the machining oils. The specimens were then heat treated for 11 hours at 2000°C (2273°K) at a pressure of approximately 5×10^{-5} mm Hg (abs) in a Brew Model 420 vacuum furnace. The temperature of the furnace had been previously calibrated by correlating the electrical input with an optical pyrometer and a thermocouple.

This particular heat treatment produced a grain diameter of 0.685 mm and altered the hydrogen, oxygen, nitrogen, and carbon content of the niobium to that given in Table I. The analysis for these elements was performed by The National Research Corporation.

2.3 Apparatus

Since the apparatus used in this investigation has previously been described in detail by other investigators,^(10, 13) only a summary of it is given here.

The mechanical apparatus used was constructed so as to apply a pure torque on one end of the specimen while holding the other end fixed. Briefly, one end of the specimen was attached to the stationary weighbar to which strain gages in the form of a Wheatstone bridge had been mounted and the other end was attached to a loading arm through which a pure torsional load was applied. The desired strain rate was produced by controlling the angular velocity of a flywheel mechanism used to contact the loading arm. In the case of the highest strain rate (12.5/sec.) the flywheel was

first accelerated to a predetermined speed by means of a friction drive motor. The motor was then disconnected. When the flywheel had slowed to the desired angular velocity, the test was begun. To develop the two slower strain rates the flywheel was driven directly by means of a motor through an appropriate number of gear reducers.

When investigating the yield behavior of niobium at the 12.5 and 0.25/sec. strain rates, the strain gages on the weighbar were connected through an amplifier to a six channel recording oscillograph. In addition to recording torque, the oscillograph also recorded the angle of twist undergone by the specimen as well as the time increments involved.

For the 0.0001/sec. strain rate, an autographic X-Y recorder was used to record the torque and angle of twist. The strain gages on the weighbar were electrically connected through an amplifier to the X-Y recorder. A potentiometer geared to the loading arm and used to detect the angle of twist of the specimen was also connected to the recorder. By driving the Y axis with the amplified strain gage signals and the X axis with the potentiometer signal, a record of the torque vs angle of twist was made.

The temperature of the specimens was controlled in one of two ways. While investigating at the elevated temperatures a resistance furnace was mounted over the specimen and while investigating at the subatmospheric temperatures a cold chamber was used in conjunction with liquid nitrogen. At the subatmospheric temperatures a means was also available whereby nitrogen could be sprayed directly onto the specimen. The temperature of the resistance furnace was controlled by an automatic temperature controller, and the temperature of the cold chamber was controlled by regulating the flow of liquid nitrogen from the storage tank to the cold chamber. In all cases a thermocouple wired to the specimen by a one mil soft wire allowed the operator to check the specimen's temperature just prior to testing. Before conducting each test, the desired temperature was held for at least two minutes to insure that a true temperature equilibrium had been reached.

3.0 RESULTS

The behavior of the upper yield point of niobium at different temperatures and strain rates as found in the present study is shown in Fig. 2. In this figure the upper yield stress is shown as a function of temperature for the three torsional strain rates used. (In order to facilitate the comparison of data from different sources, the yield stress and strain rates have been converted to octahedral terms as will be presently discussed). The specimens tested at the two highest strain rates displayed a definite upper and lower yield point. In the case of the specimens tested at the lowest strain rate, the decrease in the stress that normally follows yielding in BCC metals was not apparent. Here the upper yield point was taken to correspond to the first sharp break in the torque-angle of twist relationship.

It should be noted in Fig. 2 that at elevated temperatures the stress necessary to cause yielding becomes less sensitive to temperature. This observation has already been made in an investigation of ingot iron ^(5, 10, 12) and can be made in the case of molybdenum by examining Bechtold's ⁽¹⁾ Fig. 7 and Weinstein, et al ⁽¹¹⁾ Fig. 5. Bechtold ⁽¹⁾ also shows in his Fig. 8, a graph of the 0.01 per cent offset yield stress as a function of temperature for niobium. This graph gives evidence that the 0.01 per cent offset yield stress also becomes less dependent on temperature in much the same manner as does the upper yield stress with increased temperature.

No brittle behavior was observed in this investigation. The fracture surface of each specimen had a dull 'mattelike' appearance.

Mechanical twins were found in one specimen. While testing at the lowest temperature (77° K) and slowest strain rate (0.0001/sec.), audible clicks were heard. Subsequent examination showed twins such as those in Fig. 3.

4.0 DISCUSSION AND ANALYSIS OF RESULTS

As previously stated, it was the primary purpose of this investigation to study the influence of temperature and strain rate on the upper yield point of commercially pure niobium which had been further purified by heat treatment. Another purpose was to explore the effects of other variables on the yield behavior of niobium by analyzing other investigators' data as well as the data obtained in this investigation. The following is a systematic discussion of these variables.

4.1. The Dependence of Yield Stress on State of Stress

Since the data for this investigation was collected while the metal was subjected to a torsional state of stress and the data for the other investigations was in terms of uniaxial tension or compression, it was necessary to convert the respective yield stresses and strain rates of the individual investigations into terms having a common basis before proceeding with the analysis. To do this the von Mises theory of yielding was used.

According to the von Mises (or maximum octahedral shear stress) theory of yielding, ^(2, 3) yielding will begin in a body when the maximum shear stress on an octahedral plane reaches a critical value.

The necessary relationships between the states of stress and strain rates needed to convert the results of the individual investigations into octahedral terms are found as follows:

(a) The maximum octahedral shearing stress in terms of the principal stresses is ^(2, 3)

$$\tau_G = \frac{1}{3} \sqrt{(\sigma_1 - \sigma_2)^2 + (\sigma_2 - \sigma_3)^2 + (\sigma_1 - \sigma_3)^2} \quad (4)$$

The maximum octahedral shearing strain in terms of the principle strains is ⁽¹⁴⁾

$$\gamma_G = \frac{2}{3} \sqrt{(\epsilon_1 - \epsilon_2)^2 + (\epsilon_2 - \epsilon_3)^2 + (\epsilon_1 - \epsilon_3)^2} \quad (5)$$

(b) In a uniaxial test, $\sigma_1 = \frac{\text{load}}{\text{area}}$, $\sigma_2 = \sigma_3 = 0$, and $\epsilon_2 = \epsilon_3 = -\mu\epsilon_1$. With μ (Poisson's ratio) assumed to be 1/4 for niobium, it is found that

$$\tau_G = \frac{\sqrt{2}}{3} \sigma_1 \quad (6)$$

$$\gamma_G = \frac{5\sqrt{2}}{6} \epsilon_1 \quad (7)$$

(c) In a torsional test on a cylindrical specimen, $\sigma_1 = \tau_c = G\gamma_c$, $\sigma_2 = 0$, $\sigma_3 = -\sigma_1$, $\epsilon_1 = (1 + \mu) \frac{\sigma_1}{E}$, $\epsilon_2 = 0$, $\epsilon_3 = -\epsilon_1$ and $G = \frac{E}{2(1 + \mu)}$. (See, for example, Ref. 3 and 15) (Where: τ_c , γ_c , is the stress and strain at the distance c from the axis of a cylindrical torsion specimen, respectively; G , the modulus of rigidity; and E , Young's modulus. In this investigation, c was taken to be equal to the outside radius of the specimen).

The octahedral shearing stress for a torsional test may now be expressed in terms of the principal stresses, and the octahedral shearing strain may be expressed in terms of the principal strains. The procedure used in solving for the latter is as follows: First, substitute the above expressions for strain, i.e., ϵ_1 , ϵ_2 , and ϵ_3 , into Eq. 5; this will give $\gamma_G = f(\mu, E, \sigma_1)$. Next notice that $\sigma_1 = G\gamma_c$ and $E = 2G(1 + \mu)$. Using these relations and simple algebra will now give the results that, in the case of torsion

$$\tau_G = \frac{\sqrt{6}}{3} \tau_c \quad (8)$$

$$\gamma_G = \frac{\sqrt{6}}{3} \gamma_c \quad (9)$$

(d) Further note that if $\gamma_G = K\epsilon$, then $\frac{d}{dt}(\gamma_G) = K \frac{d}{dt}(\epsilon)$, or $\dot{\gamma}_G = K\dot{\epsilon}$, where K is a constant.

(e) The final expressions for the octahedral stresses and strains in terms of those reported for the individual investigations are:

In the case of a tensile test

$$\tau_G = \frac{\sqrt{2}}{3} \sigma, \text{ and } \dot{\gamma}_G = \frac{5\sqrt{2}}{6} \dot{\epsilon} \quad (6')(7')$$

and in the case of a torsional test

$$\tau_G = \frac{\sqrt{6}}{3} \tau_c, \text{ and } \dot{\gamma}_G = \frac{\sqrt{6}}{3} \dot{\gamma}_c \quad (8')(9')$$

With the above equations, it is possible to take the data reported by the other investigators and thereby have a common basis for comparison.

4.2 The Dependence of the Yield Stress on Temperature and Strain Rate

The next relation considered in this analysis is the rate equation. If we assume that the rate equation for the process at a given stress is (8, 9, 16)

$$\dot{\gamma}_G = A e^{\frac{-\Delta H}{RT}} \bigg|_{\tau = \text{const.}} \quad (10)$$

or,

$$\ln \dot{\gamma}_G = \ln A - \left(\frac{\Delta H}{R} \right) \frac{1}{T} \bigg|_{\tau = \text{const.}} \quad (10')$$

the simultaneous dependence of the yield stress on temperature and strain rate may be discussed.

Equation 10' shows, if the relationship exists between the given variables, that on a graph of $\ln \dot{\gamma}_G$ vs $(\frac{1}{T})$, curves representing constant yield stress should be straight lines; furthermore Eq. 10' provides a means of evaluating A for each stress level in that the intersection of each curve with the ordinate, at $\frac{1}{T} = 0$, provides the value of A.

Figure 4 presents a graph of $\ln \dot{\gamma}_G$ vs $(\frac{1}{T})$ for the data obtained in this investigation. The three lines shown are for different values of constant stress and are straight within experimental accuracy. The constant, A, obtained from the different lines appears to be independent of stress and has a value of approximately $10^4/\text{sec}$.

By rewriting Eq. 10 in terms of the stress dependent activation energy, i.e.,

$$\Delta H = RT \ln \left(\frac{A}{\dot{\gamma}_G} \right) \quad (10'')$$

and by using the stress independent value of A, one has a parametric representation of temperature and strain rate. Table I (which is subdivided into three parts: material composition, metallurgical preparation and yield data) and the accompanying Figs. 5a-5k show the relationship between the yield stress and ΔH for the material used in the present investigation as well as for the niobium used in ten other investigations⁽¹⁷⁻²⁶⁾.

This temperature-strain rate parameter provides a means of obtaining a point estimate of the effective heat of activation for the process under a given set of conditions. It is analogous to the time-temperature parameter employed by Larson and Miller⁽²⁷⁾ for stress rupture and creep studies.

4.3 The Dependence of the Yield Stress on Composition and Microstructure

The curves shown separately in Figs. 5a through 5k may be plotted on one graph. Such a graph results in a family of curves which are parallel within experimental accuracy and suggests that a common mechanism or mechanisms are operative in the yield process. The further observation that all such curves are displaced from one another in the vertical or stress direction suggest that the yield stress may be subdivided into components with composition and microstructure contributing one or more of such components.

The Petch ⁽¹⁾ equation for the lower yield stress (reported to represent ⁽¹⁹⁾ upper yield stress as well) gives a relationship which separates the observed yield stress into three components. The equation is

$$\tau_G = \tau_G(\text{st}) + \tau_G^* + kd^{-\frac{1}{2}} \quad (11)$$

This relationship postulates that τ_G should be a linear function of $d^{-\frac{1}{2}}$ and that a graph of τ_G vs $d^{-\frac{1}{2}}$ should result in a straight line relationship whose slope (i.e., $\frac{\partial \tau_G}{\partial d^{-\frac{1}{2}}}$) is k . In Fig. 6, data from two of the investigations indicate that a straight line relationship may exist between τ_G and $d^{-\frac{1}{2}}$. The different slopes, however, indicate that the value of k for niobium may also be dependent upon the composition and substructure of the material.

In view of this discrepancy in results of the effect of grain size on yield behavior a modification of Eq. 11 is required. Because the individual contributions due to grain size, composition, and substructure may not be separable from present data, their combined effects on the yield stress may as well be summarized in one component. One component (τ_{iG}) may be considered to be dependent upon the composition and microstructure of the material and assumed to be relatively insensitive to temperature and strain rate. Another component (τ_G^*) then may be assumed to be a function of temperature and strain rate only. That is

$$\tau_G = \tau_{iG} + \tau_G^* \quad (12)$$

In present terms, the vertical displacement of all the curves on a graph of τ_G vs ΔH is attributed to variations of composition and microstructure for the materials utilized in the different investigations as well as to the diversity of ways of defining yield stress.

The curves in Figs. 5a through 5k indicate that the yield stress in all investigations becomes relatively insensitive to ΔH around the value of 10 k cal/gm mol. By assuming for each particular curve that the value of yield stress which occurs at 10 k cal/gm mol is due to τ_{iG} and then subtracting this amount from the yield data in the curve, only τ_G^* remains. Furthermore, it should be mentioned that differences used to define yield stress lead to small numerical differences in the value of yield stress at any particular value of ΔH . The resulting curves, however, are parallel and differ primarily by a small constant amount in the term τ_{iG} . Specifically, by adjusting the yield data from the individual curve in every investigation an amount equal to the stress at ΔH equal to 10 k cal/gm mol to account for differences in composition and microstructure as well as differences arising from the various definitions for yield stress, a common representation of the effect of ΔH on τ_G^* is made possible as shown in Fig. 7. This figure summarizes data obtained in the eleven investigations and shows, within experimental accuracy, that the dependence of τ_G^* on ΔH is non-linear and is similar for all investigations. It should be noted that the activation volume may be obtained from Fig. 7 by the relationship $\frac{\partial \tau_G}{\partial \Delta H} = \frac{1}{V}$.

In Fig. 7 it is apparent that the influence of ΔH on τ_G^* suddenly changes around 10 k cal/gm mol. Also in Fig. 7 the mean value of τ_G^* appears to become negative for values of ΔH larger than about 10 k cal/gm mol when it may be expected to remain at zero. This is a consequence of the temperature dependence of the component τ_{iG} which decreases directly with the temperature dependence of the elastic modulus of the material. For purposes of the present paper it is not considered necessary to include this small correction in presenting the data.

The data presented in this paper covers a temperature range of more than 1000° K and a strain rate range of approximately six orders of magnitude. Also three different states of stress are reported and over eleven different niobium materials are represented. It appears feasible from Fig. 7 to assume that the yielding relation in terms of the variables presented may be given by

$$\dot{\gamma}_G = A e^{-\frac{[\Delta H^* - V(\tau_G - \tau_{iG})]}{RT}} \quad (13)$$

5.0 SUMMARY AND CONCLUSIONS

The yield behavior of niobium has been examined in terms of pertinent engineering variables. The particular variables considered in this paper are state of stress, temperature, strain rate, and composition and microstructure of the material.

For ductile niobium, the von Mises criterion (maximum octahedral shear stress) for yielding describes a variety of data obtained under conditions of uniaxial tension, compression, and torsional loading. The data summarized herein includes results from some 250 specimens subjected to a temperature range of more than 1000°K and a strain rate variation of approximately six orders of magnitude.

The frequency factor A in the modified form of the rate equation,

$\dot{\gamma} = A e^{\frac{-\Delta H}{RT}}$, appears to be independent of stress and has a value for niobium of approximately $10^4/\text{sec}$ (Fig. 4). By rewriting the rate equation in terms of ΔH , a parameter for temperature and strain rate is formed which makes possible the simultaneous representation of the dependence of the yield stress on the two variables. This dependence is found to be similar for all data reported (Figs. 5a through 5k).

The method of analysis which is used in this paper separates the observed yield stress into two components: one component (τ_{iG}) is considered dependent on the composition and microstructure of the material and assumed to be relatively insensitive to temperature and strain rate, the other component (τ_G^*) is assumed to be a function of temperature and strain rate alone. In the region $\Delta H < 10 \text{ k cal/gm mol}$, τ_G^* is very sensitive to changes in ΔH (Fig. 7). At values of ΔH greater than this the mechanism of yielding appears to change radically and the yield stress becomes relatively independent of changes in temperature and strain rate.

By using data from eleven investigations, this analysis shows that the dependence of stress on the above variables for relatively pure niobium may be given by the following relationship:

$$\dot{\gamma}_G = A e^{\frac{-[\Delta H^* - V(\tau_G - \tau_{iG})]}{RT}} \quad (12)$$

6.0 REFERENCES

1. B. L. Averbach, et al., Fracture, The Technology Press, M.I.T. and John Wiley and Sons, Inc., New York (1959).
2. O. Hoffman and G. Sachs, Introduction to the Theory of Plasticity for Engineers, McGraw-Hill Book Company, Inc., New York (1953), pp. 3-20, 28, and 39-40.
3. F. B. Seely and J. O. Smith, Advanced Mechanics of Materials, Second Edition, Third Printing, John Wiley and Sons, Inc., New York (1957), pp. 61-64, 67, 81-82 and 89-90.
4. Hans Conrad, "On the Mechanism of Yielding and Flow in Iron," Journal of the Iron and Steel Institute, Vol. 198, August, 1961.
5. Hans Conrad and S. Frederick, "The Effect of Temperature and Strain Rate on the Flow Stress of Iron," To appear in Acta-Met.
6. Hans Conrad, "Yielding and Flow in Iron," To appear in AIME/Interscience - Wiley Metallurgical Conference Volume entitled "High Purity Iron and Its Dilute Solid Solutions".
7. Hans Conrad and W. Hayes, "Thermally-Activated Deformation of the B.C.C. Metals at Low Temperatures," Submitted to Transactions ASM.
8. I.I. Betcherman, "Rate Processes in Physical Metallurgy," "Progress in Metal Physics," Vol. 2, 1950.
9. E. Kauzmann, "Flow of Solid Metals from the Standpoint of Chemical Rate Theory," Trans. AIME (Metals Division), Vol. 143, 1941.
10. P. E. Bennett and G. M. Sinclair, "An Analysis of the Time and Temperature Dependence of the Upper Yield Point in Iron," ASME Technical Paper No. 61-Met-1, (April 1961).
11. D. Weinstein, G. M. Sinclair and C. A. Wert, "The Strain Rate and Temperature Dependence of the Ductile to Brittle Transition in Molybdenum Subjected to Torsional Loading," University of Illinois, TAM Report No. 156, (December 1959).
12. P. E. Bennett and G. M. Sinclair, "Parameter Representation of the Yield Behavior of Iron," ASME, Paper No. 62-WA-263, 1962.
13. C. E. Work and T. J. Dolan, "The Influence of Temperature and Rate of Strain on the Properties of Metals in Torsion," University of Illinois Engineering Experiment Station, Bulletin No. 420, (1953).
14. M. Hetenyi, ed., Handbook of Experimental Stress Analysis, John Wiley and Sons, Inc., New York (1950), p. 5.
15. S. Timoshenko and J. N. Goodier, Theory of Elasticity, McGraw Hill Book Company Inc., New York, (1951) p. 5.
16. M. Sinnott, The Solid State for Engineers, John Wiley and Sons, Inc, New York (1958), pp. 86- 104.

17. E. Wessel and D. Lawthers, "The Ductile to Brittle Transition in Niobium," Westinghouse Scientific Paper No. 6-94701-5-P1. Westinghouse Research Laboratories, Pittsburgh, Pennsylvania.
18. M. A. Adams, A. C. Roberts, and R. E. Smallman, "Yield and Fracture in Polycrystalline Niobium," *Acta Met.*, Vol. 8, No. 5 (May 1960) pp. 328-ff.
19. E. S. Tankins and R. Maddin, "Effect of Grain Size, Strain Rate and Temperature on the Yield Strength of Columbium," AIME Columbium Metallurgical Symposium, Lake George, New York, (June 9-10, 1960). (Data taken from uncorrected preprints of the manuscript as published by Interscience Publishers, Inc. New York).
20. B. F. Dyson, R. B. Jones and W. J. Mc G. Tegart, "The Tensile Properties of High Purity Niobium at Low Temperature," *Journal, Institute of Metals*, Vol. 87, p. 340 (1958-59).
21. B. A. Wilcox, A. W. Brisbane and R. F. Klinger, "The Effects of Strain Rate and Hydrogen Content on the Low Temperature Deformation Behavior of Columbium," WADD Technical Report No. 61-44 (Preprint), May 1961.
22. A. L. Mincher and W. F. Sheely, "Effect of Structure and Purity on the Mechanical Properties of Columbium," *Trans. of Met. Soc. of AIME*, Vol. 221, No. 1, pp. 19-25 (February 1961).
23. R. T. Begley and L. L. France, "Effect of Oxygen and Nitrogen on Workability and Mechanical Properties of Columbium," STP 272, ASTM, Symposium on Newer Metals, 1961.
24. A. T. Churchman, "Cleavage Fracture in Niobium," *Journal, Institute of Metals* Vol. 88, pp. 221-222, 1959-60.
25. A. A. Johnson, "The Low Temperature Tensile Properties of Niobium," *Acta Met.*, Vol. 8, No. 10, pp. 737-740, October 1960.
26. E. T. Wessel, L. L. France, and R. T. Begley, "The Flow and Fracture Characteristics of Electron Beam Melted Columbium," Westinghouse Scientific Paper No. 11-0103-1, P 1, Westinghouse Research Laboratories, Pittsburgh, Pennsylvania. July 1960.
27. F. R. Larson and J. Miller, "A Time-Temperature Relationship for Rupture and Creep Stress," *Trans. ASME*, Vol. 74, (1952) pp. 765-ff.

7.0 APPENDIX

Definition of Terms

τ	shear stress (applied)
τ_G	maximum octahedral shear stress
τ_i	internal (frictional) stress
τ_{iG}	internal (frictional) stress in octahedral terms
$\tau_G^{(st)}$	internal (frictional) stress dependent upon composition and sub-structure but independent of grain size
τ^*	temperature and strain rate dependent component of the yield stress
τ_G^*	temperature and strain rate dependent component of the yield stress in octahedral terms
γ	shear strain
γ_G	maximum octahedral shear strain
$\dot{\gamma}$	shear strain rate, i.e., $\frac{d\gamma}{dt}$
$\dot{\gamma}_G$	maximum octahedral shear strain rate
ΔH	effective activation energy (stress dependent)
ΔH^*	effective activation energy at zero stress
A	frequency factor
d	grain diameter in mm
e	base of natural logarithms
k	slope of yield stress vs $d^{-\frac{1}{2}}$
R	universal gas constant
T	temperature in $^{\circ}\text{K}$
V	activation volume

TABLE Ia MATERIAL COMPOSITIONS FOR INVESTIGATIONS INCLUDED IN THIS REPORT (wt. %)

Investigation Present	H	O	N	C	Zr	Ta	Fe	Ni	W	Ti	Si	Others
Investigation	0.000023	0.0007	0.0068	0.0093	0.02	0.02	0.02	0.01	0.01	0.02		
17a		0.021	0.012	0.0114	0.10	0.338						
17b		0.014	0.018	0.0143	0.10	0.338						
18	0.02	0.01	0.05	0.07		0.30	0.30				0.150	0.03
19	0.0005	0.006	0.005	0.02		0.16				0.005	0.015	
20		0.007		0.01		<0.3	<0.08		Trace			
21a	0.0001	0.0317	0.065	0.009								
21b	0.0009	0.042	0.021	0.013								
21c	0.0030	0.039	0.0085	0.014								
22a	0.0008	0.010	0.009	0.021	<0.015	≈0.1	<0.015			<0.015	<0.015	B<0.0001
22b	<0.001	0.040	0.034	0.037	<0.015	≈0.1	<0.015			<0.015	<0.015	B<0.0001
22c	<0.001	0.040	0.020	0.030	<0.015	≈0.1	<0.015			<0.015	<0.015	B<0.0001
22d	<0.001	0.040	0.010	0.027	<0.015	≈0.1	<0.015			<0.015	<0.015	B<0.0001
23a		0.067	0.024	0.012		0.05						
23b		0.020	0.026	0.02		0.07						
23c		0.0030	0.002	0.024- 0.068								
24		0.04- 0.05										
25	0.0014	0.034	0.014	0.01	<0.1	<0.3	<0.01			<0.01	<0.01	Co<0.01
							0.03			0.05	0.01	K<0.002 Sn<0.005 Pb<0.005 Na<0.002
26	0.0001	0.020	0.011	0.018	<0.03	0.20	0.004			0.17	0.02	

TABLE Ib. GRAIN SIZES AND HEAT TREATMENTS

Investigation	Grain Diameter	Final Heat Treatment
Present Investigation	0.095 mm	11 hr at 2,000°C in a vacuum of approx. 5×10^{-5} mm Hg.
17a	0.5 mm	2 hr at 1,200°C in a vacuum of less than 1×10^{-5} mm Hg.
17b	0.5 mm	2 hr at 1,200°C in a vacuum of less than 5×10^{-6} mm Hg.
18a	1.414 mm	2 hr at 1,415°C in a vacuum of 10^{-5} - 10^{-6} mm Hg.
18b	0.0476 mm	1 hr at 1,190°C in a vacuum of 10^{-5} - 10^{-6} mm Hg.
19a	0.0635 mm	$\frac{1}{2}$ hr at 1,000°C in a dynamic vacuum
19b	0.127 mm	1 hr at 1,000°C in a dynamic vacuum
19c	0.3175 mm	1 hr at 1,200°C in a dynamic vacuum
20	0.01414 mm	2 hr at 1,200°C in a vacuum of less than 10^{-4} mm Hg.
21a	0.041 mm	As received (arc-melted)
21b	0.041 mm	Hydrogen anneal 3 hr at 400°C then Argon anneal 4 hr at 400°C
21c	0.041 mm	Hydrogen anneal 6 hr at 400°C then Argon anneal 6 hr at 400°C (in all cases-Final H. T. was prior to machining)
22a	0.045 mm	2 hr at 1,093°C
22b	0.022 mm	1 hr at 1,200°C
22c	0.022 mm	3 hr at 1,065°C
22d	0.022 mm	3 hr at 1,065°C
23a	0.180 mm	all material in completely recrystallized condition
23b	0.065 mm	"
23c	<0.250 mm	"
24a	0.41 mm	1,200-2,000°C in a vacuum
24b	0.013 mm	1,200-2,000°C in a vacuum
24c	0.017 mm	1,200-2,000°C in a vacuum
25	0.037 - 0.0138 mm	1,100-2,300°C in a vacuum
26	0.095 mm	2 hr at 1,200°C in a vacuum

TABLE Ic TABULATED YIELD DATA

Investigation	Type of Investigation	Criterion for yielding	Temp ($^{\circ}$ K)	Octahedral Yield Stress kg/mm ²	Octahedral Strain Rate, $\dot{\gamma}_G$ (1/sec)	$\Delta H = RT \ln \frac{A}{\dot{\gamma}_G}$ (cal/gm mole)
Present Investigation	Torsion	Upper Yield Stress	77	24.5	8.16×10^{-5}	2,800
			77	23.0	"	2,800
			105	23.2	"	3,800
			122	18.5	"	4,400
			156	18.4	"	5,700
			168	14.1	"	6,200
			199	11.1	"	7,300
			225	7.2	"	8,300
			257	5.6	"	9,450
			298	4.8	"	11,100
			77	24.0	0.204	1,630
			113	27.1	"	2,400
			150	23.0	"	3,180
			175	18.5	"	3,710
			213	15.7	"	4,520
			249	12.7	"	5,280
			299	9.3	"	6,340
			351	7.0	"	7,440
			400	5.5	"	8,480
			77	37.7	10.2	1,000
			77	36.4	10.2	1,030
			94	34.7	10.2	1,260

TABLE Ic. (cont)

Investigation	Type of Investigation	Criterion for yielding	Temp ($^{\circ}$ K)	Octahedral Yield Stress kg/mm ²	Octahedral Strain Rate, $\dot{\gamma}_G$ (1/sec)	$\Delta H = RT \ln \frac{A}{\dot{\gamma}_G}$ (cal/gm mole)
Present Investigation	Torsion	Upper Yield Stress	130	34.6	10.2	1,740
			148	34.0	"	1,980
			170	29.4	"	2,280
			197	28.2	"	2,640
			246	20.6	"	3,290
			251	27.1	"	3,360
			277	21.2	"	3,710
			296	20.2	"	3,960
			298	19.0	"	3,990
			339	16.8	"	4,540
			373	13.6	"	4,990
			418	11.3	"	5,590
			463	10.1	"	6,200
			521	8.2	"	6,970
			580	5.9	"	7,760
			148	22.2	1.18 x 10 ⁻³	4,720
			173	18.9	"	5,520
17a	Tension	Upper Yield Stress	223	14.2	"	7,110
			298	9.9	"	9,510
			77	36.8	1.31 x 10 ⁻²	2,090
			123	28.0	"	3,330

TABLE Ic. (cont)

Investigation	Type of Investigation	Criterion for yielding	Temp ($^{\circ}$ K)	Octahedral Yield Stress kg/mm ²	Octahedral Strain Rate (1/sec)	$\dot{\gamma}_G$	$\Delta H = RT \ln \frac{A}{\dot{\gamma}_G}$ (cal/gm mole)
17b	Tension	Upper Yield Stress	173	21.4	1.31×10^{-2}		4,690
			223	15.9	"		6,040
18a	Tension	Upper Yield Stress	20	39.0	2.38×10^{-4}		700
			77	32.8	"		2,700
			77	36.8	7.30×10^{-2}		1,820
			195	14.5	2.38×10^{-4}		6,840
			293	6.9	"		10,280
18b			20	38.0	"		700
			77	38.8	7.30×10^{-2}		1,820
			77	33.4	2.38×10^{-4}		2,700
			195	15.2	"		6,840
			293	7.9	"		10,280
19a	Tension	Upper Yield Stress	90	52.9	7.79×10^{-2}		2,100
			90	45.4	7.79×10^{-3}		2,550
			90	43.4	3.89×10^{-3}		2,650
			90	41.5	7.79×10^{-4}		2,950
			90	37.8	3.89×10^{-4}		3,050
			90	36.4	1.97×10^{-4}		3,200
			223	27.5	2.07×10^{-2}		5,850
			223	24.8	3.89×10^{-3}		6,550
			223	23.2	1.65×10^{-3}		6,950
			223	22.4	8.26×10^{-4}		7,250

TABLE Ic (cont)

Investigation	Type of Investigation	Criterion for yielding	Temp (°K)	Octahedral Yield Stress kg/mm ²	Octahedral Strain Rate, $\dot{\gamma}_G$ (1/sec)	$\Delta H = RT \ln \frac{A}{\dot{\gamma}_G}$ (cal/gm mole)
19a	Tension	Upper Yield Stress	223	20.9	4.40×10^{-4}	7,550
			223	19.4	1.97×10^{-4}	7,900
			296	22.5	1.97×10^{-2}	7,750
			296	20.0	3.89×10^{-3}	8,700
			296	19.2	1.97×10^{-3}	9,100
			296	15.9	7.79×10^{-4}	9,700
			296	15.2	3.89×10^{-4}	10,100
			296	13.1	1.97×10^{-4}	10,500
			90	39.4	3.78×10^{-2}	2,250
			90	38.0	1.97×10^{-2}	2,350
			90	36.0	7.79×10^{-3}	2,550
			90	36.4	3.89×10^{-3}	2,650
			90	33.8	1.97×10^{-3}	2,800
			90	29.9	7.79×10^{-4}	2,950
19b	Tension	Upper Yield Stress	90	27.2	3.89×10^{-4}	3,050
			90	26.8	1.97×10^{-4}	3,200
			223	20.0	5.90×10^{-2}	5,350
			223	20.9	2.07×10^{-2}	5,850
			223	17.2	2.07×10^{-2}	5,850
			223	16.5	7.79×10^{-3}	6,250
			223	14.5	3.89×10^{-3}	6,500
			233	13.7	1.65×10^{-3}	6,950

TABLE 1c (cont)

Investigation	Type of Investigation	Criterion for yielding	Temp (°K)	Octahedral Yield Stress kg/mm ²	Octahedral Strain Rate, $\dot{\gamma}_G$ (1/sec)	$\Delta H = RT \ln \frac{A}{\dot{\gamma}_G}$ (cal/gm mole)
19b	Tension	Upper Yield Stress	223	14.0	8.26×10^{-4}	7,250
			223	13.2	8.26×10^{-4}	7,250
			223	12.6	4.43×10^{-4}	7,550
			223	11.4	1.97×10^{-4}	7,900
			296	10.3	1.97×10^{-2}	7,750
			296	9.1	7.79×10^{-3}	8,300
			296	8.9	3.89×10^{-3}	8,700
			296	7.8	1.97×10^{-3}	9,100
			296	7.5	7.79×10^{-4}	9,700
			296	7.3	3.89×10^{-4}	10,100
			296	6.5	1.97×10^{-4}	10,500
			90	34.7	3.78×10^{-2}	2,250
			90	32.4	1.97×10^{-2}	2,350
			90	28.8	7.79×10^{-3}	2,550
			90	26.5	3.89×10^{-3}	2,650
			90	27.2	1.97×10^{-3}	2,800
19c			90	24.8	7.79×10^{-4}	2,950
			90	23.6	3.89×10^{-4}	3,050
			90	23.5	1.97×10^{-4}	3,200
			223	12.2	2.07×10^{-2}	5,850
			223	11.1	7.79×10^{-3}	6,250
			223	10.8	3.89×10^{-3}	6,500

TABLE Ic (cont)

Investigation	Type of Investigation	Criterion for yielding	Temp (°K)	Octahedral Yield Stress kg/mm ²	Octahedral Strain Rate, $\dot{\gamma}_G$ (1/sec)	$\Delta H = RT \ln \frac{A}{\dot{\gamma}_G}$ (cal/gm mole)
19c	Tension	Upper Yield Stress	223	9.8	1.65×10^{-3}	6,950
			223	9.8	8.26×10^{-4}	7,250
			223	9.4	4.43×10^{-4}	7,550
			223	8.4	1.97×10^{-4}	7,900
			296	7.5	1.97×10^{-2}	7,750
			296	6.6	7.79×10^{-3}	8,300
			296	6.1	3.89×10^{-3}	8,700
			296	5.6	1.97×10^{-3}	9,100
			296	5.5	7.79×10^{-4}	9,700
			296	5.0	3.89×10^{-4}	10,100
			296	4.6	1.97×10^{-4}	10,500
			77	37.1	7.90×10^{-5}	2,870
			151	20.6	"	5,620
20	Tensile	Upper Yield Stress	195	12.7	"	7,260
			294	7.6	"	9,100
			369	5.3	"	13,750
			415	5.3	"	15,480
			454	4.7	"	16,900
			513	4.7	"	19,100
			78	44.5	1.97×10^{-3}	2,400
21a	Tensile	.2% Offset	123	35.4	"	3,800
			168	34.1	9.83×10^{-5}	6,200

TABLE Ic (cont)

Investigation	Type of Investigation	Criterion for yielding	Temp (°K)	Octahedral Yield Stress kg/mm ²	Octahedral Strain Rate, $\dot{\gamma}_G$ (1/sec)	$\Delta H = RT \ln \frac{A}{\dot{\gamma}_G}$ (cal/gm mole)
21a	Tensile	.2% Offset	168	21.2	9.83×10^{-5}	6,200
			195	21.4	1.97×10^{-5}	6,000
			223	15.2	9.83×10^{-5}	8,200
			298	15.1	1.97×10^{-5}	9,200
			298	12.1	9.83×10^{-5}	10,100
21b	Tensile	.2% Offset	78	43.6	"	2,900
			123	32.8	"	4,500
			195	24.9	"	7,200
			223	23.0	"	8,200
			298	16.3	"	10,100
			78	45.8	"	2,900
			123	35.6	"	4,500
			195	23.2	"	7,200
21c	Tensile	.2% Offset	223	26.2	"	8,200
			243	23.2	"	8,950
			298	16.6	"	10,100
			79	33.9	9.84×10^{-6}	3,270
			179	12.3	"	7,410
			285	7.5	"	11,800
			386	5.8	"	16,000
			572	4.7	"	23,700
			677	5.3	"	28,050
22a	Tensile	.2% Offset				

TABLE Ic (cont)

Investigation	Type of Investigation	Criterion for yielding	Temp (°K)	Octahedral Yield Stress kg/mm ²	Octahedral Strain Rate, $\dot{\gamma}_G$ (1/sec)	$\Delta H = RT \ln \frac{A}{\dot{\gamma}_G}$ (cal/gm mole)
22a	Tensile	.2% Offset	808	4.0	9.84×10^{-6}	33,450
			1080	2.4	"	44,750
22b			75	35.7	9.84×10^{-6}	3,100
			184	18.6	"	7,620
			283	11.2	"	11,720
			573	9.4	"	23,750
			870	5.0	"	36,000
			1129	2.7	"	46,750
22c			289	13.2	9.84×10^{-6}	12,000
			535	10.7	"	22,180
			663	5.3	"	27,450
			783	4.4	"	32,400
			804	4.4	"	33,300
			934	2.6	"	38,700
22d			309	12.3	9.84×10^{-6}	12,800
			535	9.1	"	22,180
			670	6.3	"	27,800
			885	3.1	"	36,650
			1081	2.8	"	44,800
23a	Tensile	.2% Offset	77	30.8	1.18×10^{-3}	2,460
			173	25.3	"	5,520
			224	19.7	"	7,150

TABLE Ic (cont)

Investigation	Type of Investigation	Criterion for yielding	Temp (°K)	Octahedral Yield Stress kg/mm ²	Octahedral Strain Rate, $\dot{\gamma}_G$ (1/sec)	$\Delta H = RT \ln \frac{A}{\dot{\gamma}_G}$ (cal/gm mole)
23a	Tensile	.2% Offset	297	14.8	1.18×10^{-3}	9,460
23b			522	9.9	"	16,650
			77	29.8	"	2,460
			194	13.1	"	6,180
23c			297	6.6	"	9,460
			77	25.2	"	2,460
			224	7.9	"	7,150
24a	Tensile	Lower Yield Stress	297	3.8	"	9,460
			93	31.8	4.92×10^{-4}	3,100
			195	17.8	"	6,550
24b			195	14.6	"	6,550
			293	9.1	"	9,850
			293	7.6	"	9,850
24c			93	29.8	"	3,100
			195	17.8	"	6,550
			293	11.6	"	9,850
25	Tension	Proportional Limit	93	33.8	"	3,100
			93	30.6	"	3,100
			195	15.3	"	6,550
25.			293	11.6	"	9,850
			293	9.1	"	9,850
			76	35.5	1.04×10^{-4}	2,790

TABLE Ic (cont)

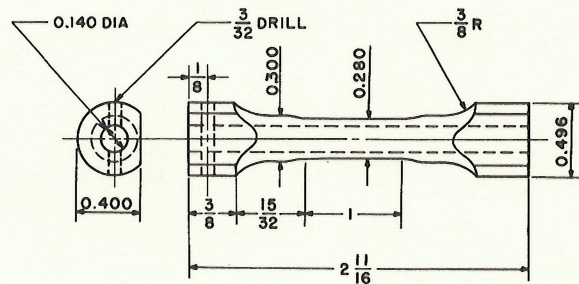
Investigation	Type of Investigation	Criterion for yielding	Temp (°K)	Octahedral Yield Stress kg/mm ²	Octahedral Strain Rate, $\dot{\gamma}_G$ (1/sec)	$\Delta H = RT \ln \frac{A}{\dot{\gamma}_G}$ (cal/gm mole)
25	Tension	Proportional Limit	76	33.8	1.04×10^{-4}	2,790
			76	32.7	"	"
			76	33.2	"	"
			76	33.8	"	"
			76	33.9	"	"
			195	14.8	"	7,150
			195	13.9	"	"
			195	13.5	"	"
			195	15.5	"	"
			195	13.1	"	"
			293	8.6	"	10,750
			293	7.9	"	"
			293	8.3	"	"
26	Tensile	.01% Offset	293	6.8	"	"
			293	7.2	"	"
			293	8.6	"	"
			44	37.8	1.18×10^{-3}	1,400
			59	34.2	"	1,900
			78	31.0	"	2,500
			78	28.7	"	2,500
			78	27.8	"	2,500

TABLE Ic (cont)

Investigation	Type of Investigation	Criterion for yielding	Temp (°K)	Octahedral Yield Stress kg/mm ²	Octahedral Strain Rate, $\dot{\gamma}_G$ (1/sec)	$\Delta H = RT \ln \frac{A}{\dot{\gamma}_G}$ (cal/gm mole)
26	Tensile	.01% Offset	126	22.4	1.18 x 10 ⁻³	4,000
			150	18.9	"	4,800
			174	17.4	"	5,550
			253	11.8	"	8,100
			298	8.6	"	9,500
			298	7.7	"	9,500
			373	5.9	"	11,900
			473	5.2	"	15,100
			573	4.4	"	18,300
			673	3.9	"	21,400
			773	2.9	"	24,600
			873	1.6	"	27,800
	Compression	0.05% Offset	77	32.6	1.18 x 10 ⁻⁴	2,800
			120	23.5	"	4,400
			220	12.3	"	8,050
			296	8.2	"	10,800
			369	7.5	"	13,500
			471	5.8	"	17,200
			521	5.2	"	19,000
			571	4.9	"	20,800
			671	3.7	"	24,500

TABLE Ic (cont)

Investigation	Type of Investigation	Criterion for yielding	Temp (°K)	Octahedral Yield Stress kg/mm ²	Octahedral Strain Rate, $\dot{\gamma}_G$ (1/sec)	$\Delta H = RT \ln \frac{A}{\dot{\gamma}_G}$ (cal/gm mole)
26	Compression	0.05% Offset	721	3.3	1.18×10^{-4}	26,400
			773	2.9	"	28,200
			4	37.8	1.18×10^{-3}	125
			4	38.2	"	125
			48	38.8	"	1,500
			78	36.4	"	2,500
			99	33.0	"	3,150
			126	26.0	"	4,000
			150	23.0	"	4,800
			173	20.5	"	5,500
			223	15.1	"	7,100
			258	11.5	"	8,250
			298	9.2	"	9,500
			373	7.8	"	11,900
			473	6.4	"	15,100



Note: All Dimensions in Inches.

FIG.1 THE GEOMETRY OF THE TORSION SPECIMENS

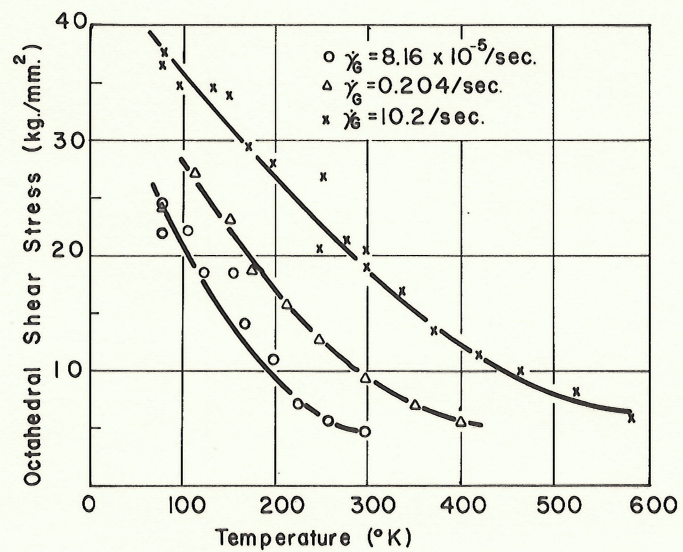
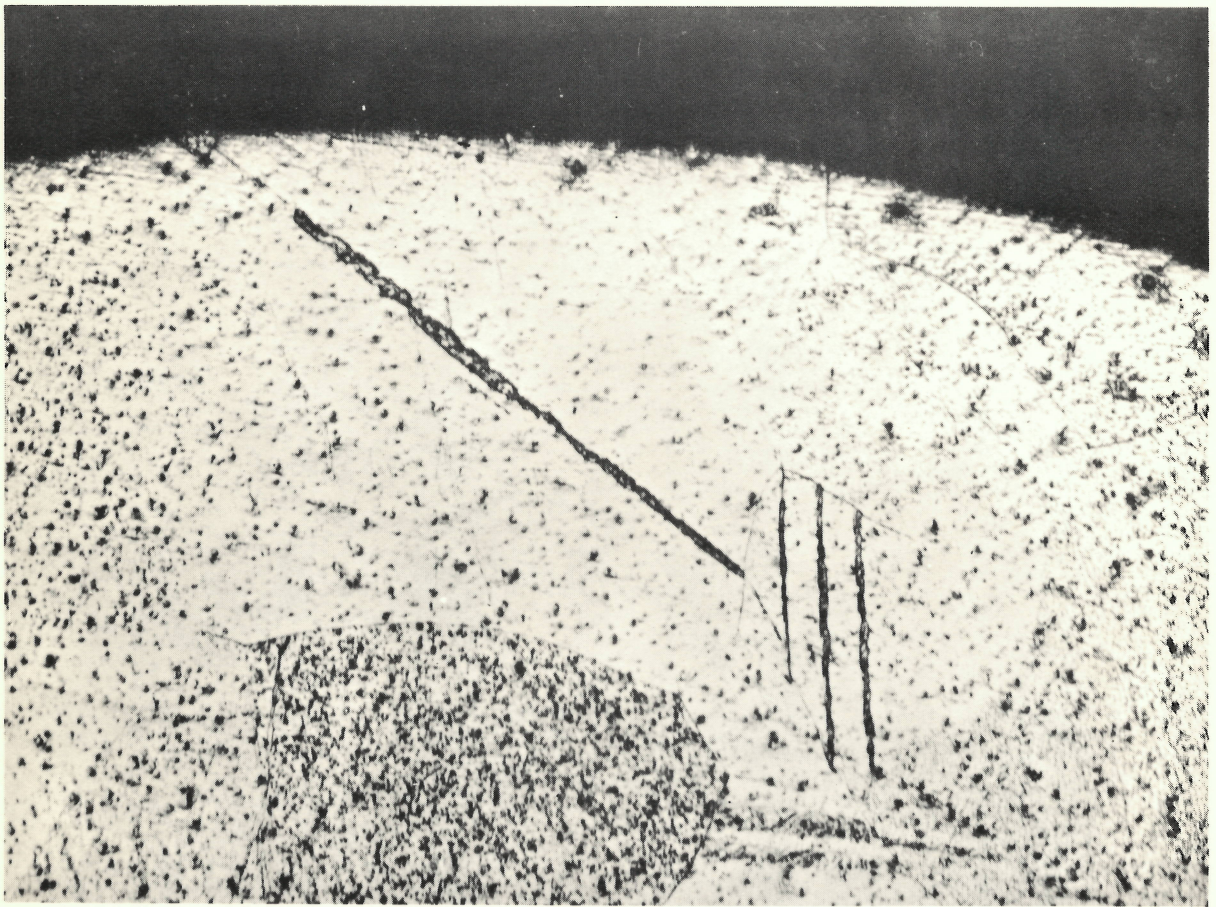


FIG.2 EFFECT OF STRAIN RATE AND TEMPERATURE ON UPPER YIELD POINT OF NIOBIUM (PRESENT INVESTIGATION)



Etchant: 10% HF+90% HNO₃ at 80°C X100

FIG. 3 PHOTOMICROGRAPH OF SPECIMEN LOADED
AT $\dot{\epsilon} = 0.0001$ / sec., T=77° K

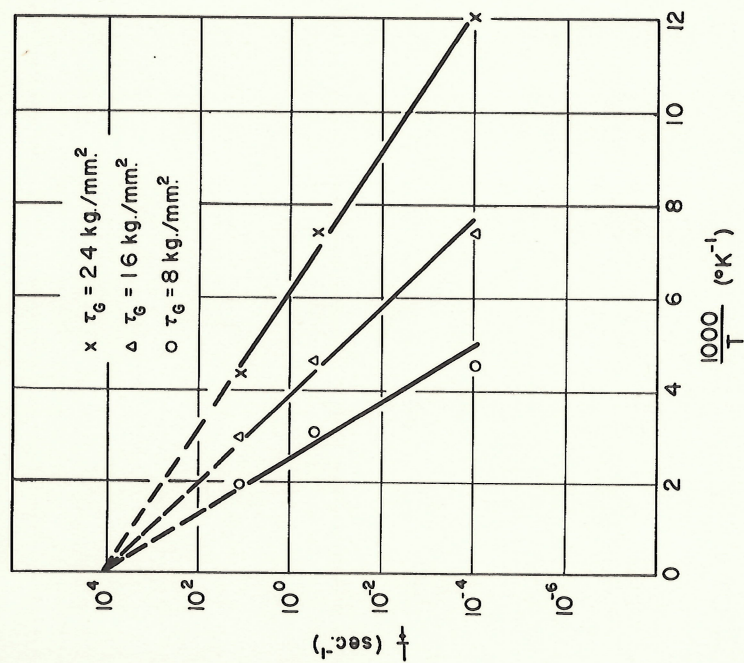


FIG.4 FREQUENCY FACTOR, A, AS DETERMINED FROM STRAIN RATE AND TEMPERATURE DEPENDENCE OF YIELD POINT IN NIOBIUM (PRESENT INVESTIGATION)

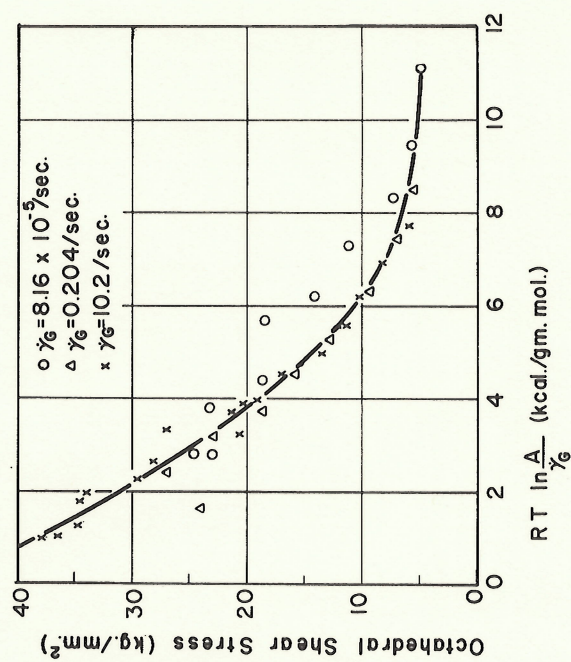


FIG.5a UPPER YIELD STRESS AS A FUNCTION OF TEMPERATURE AND STRAIN RATE FOR TORSION DATA (PRESENT INVESTIGATION)

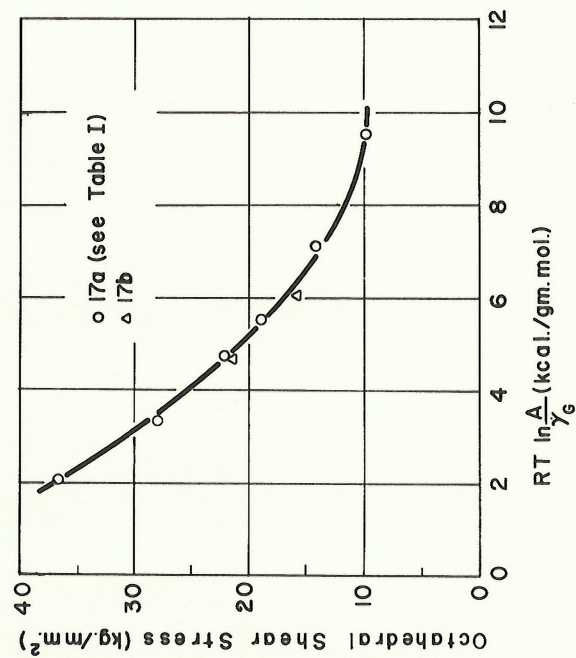


FIG.5b UPPER YIELD STRESS AS A FUNCTION OF TEMPERATURE AND STRAIN RATE FOR TENSILE DATA (WESSEL AND LAWTHERS, 17)

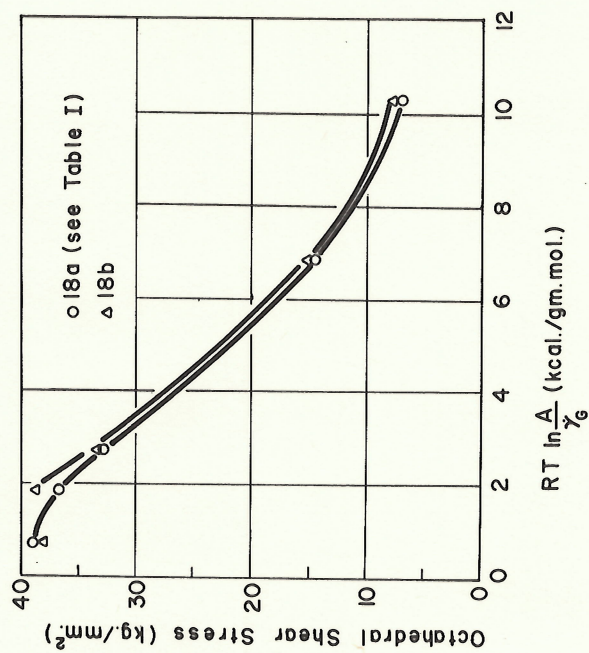


FIG.5c UPPER YIELD STRESS AS A FUNCTION OF TEMPERATURE AND STRAIN RATE FOR TENSILE DATA (ADAMS, ROBERTS AND SMALLMAN, 18)

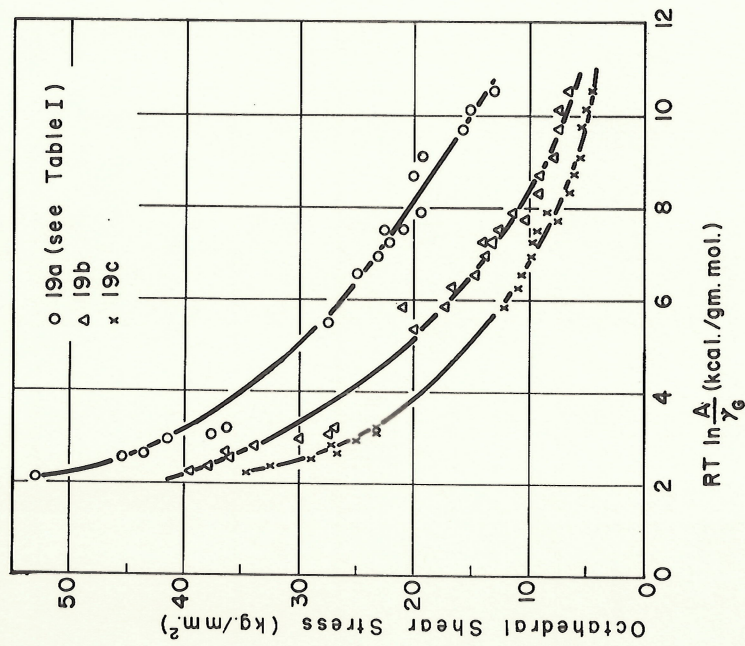


FIG.5d UPPER YIELD STRESS AS A FUNCTION OF TEMPERATURE AND STRAIN RATE FOR TENSILE DATA (TANKINS AND MADDIN, 19)

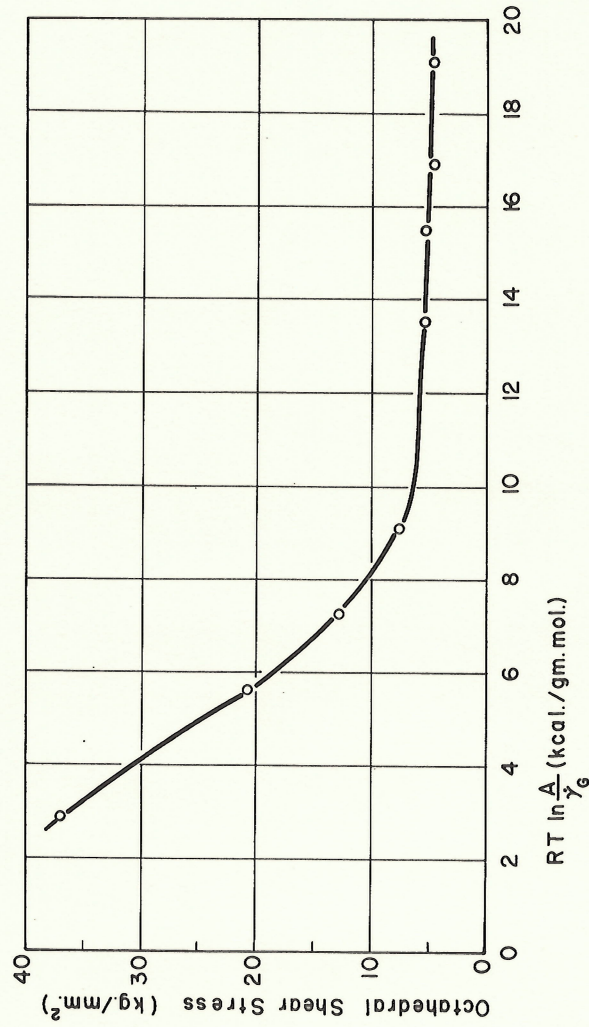


FIG.5e UPPER YIELD STRESS AS A FUNCTION OF TEMPERATURE AND STRAIN RATE FOR TENSILE DATA (DYSON, JONES AND TEGART, 20)

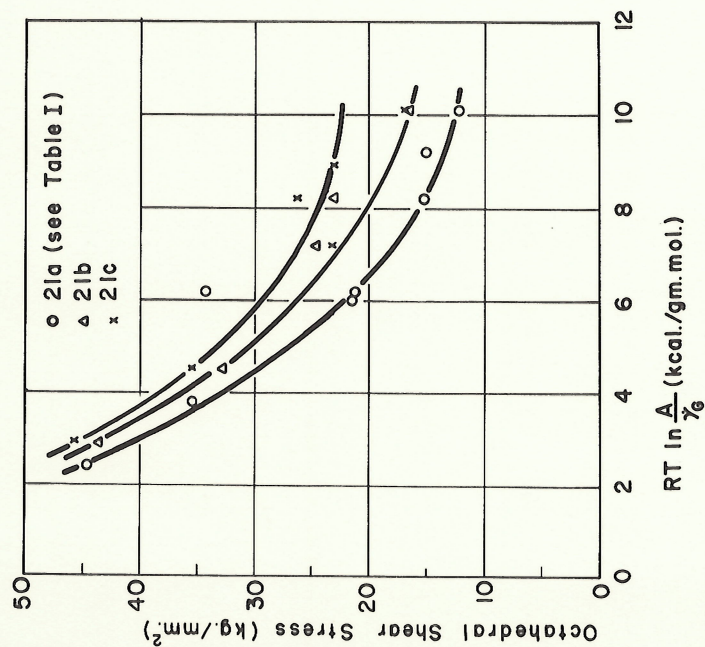


FIG.5f 0.2% OFFSET YIELD STRESS AS A FUNCTION OF TEMPERATURE AND STRAIN RATE FOR TENSILE DATA (WILCOX, BRISBANE AND KLINGER, 21)

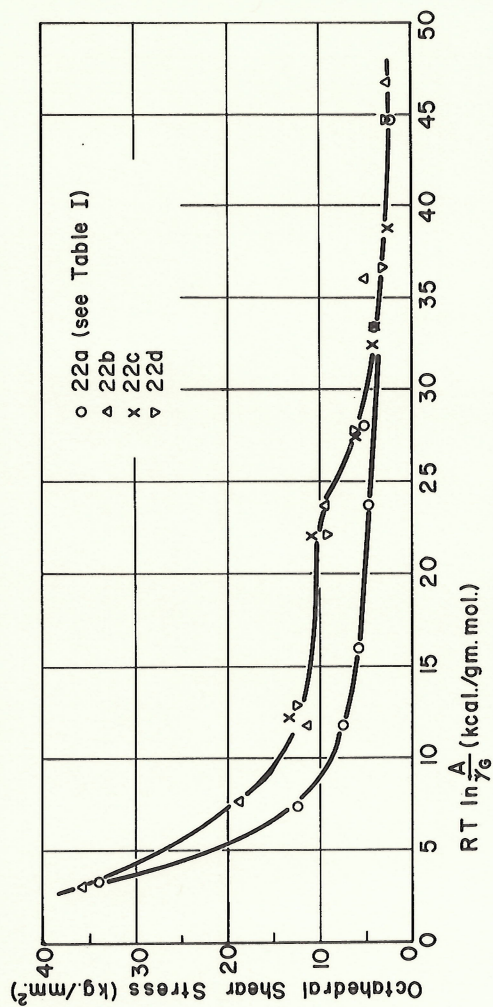


FIG.5g 0.2% OFFSET YIELD STRESS AS A FUNCTION OF TEMPERATURE AND STRAIN RATE FOR TENSILE DATA (MINCHER AND SHEELY, 22)

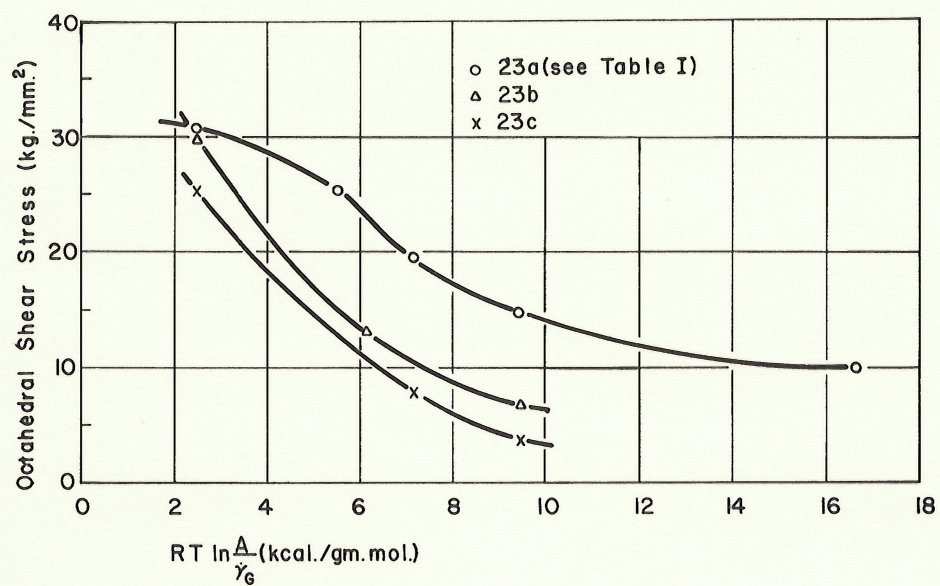


FIG.5h 0.2% OFFSET YIELD STRESS AS A FUNCTION OF TEMPERATURE AND STRAIN RATE FOR TENSILE DATA (BEGLEY AND FRANCE, 23)

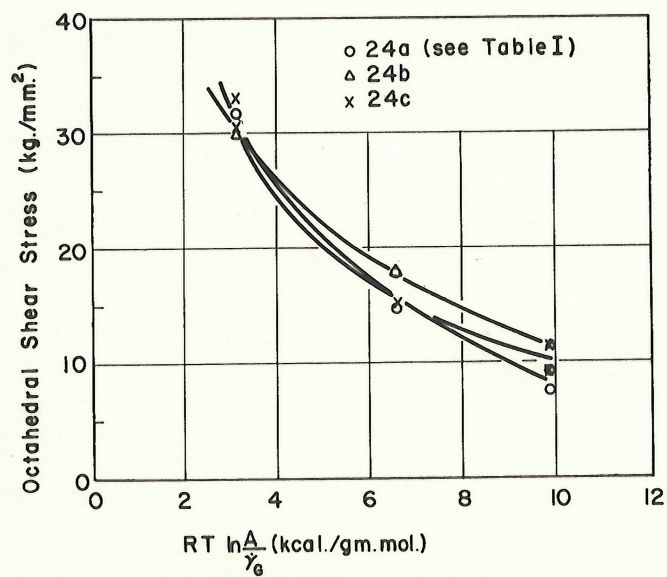


FIG.5i LOWER YIELD STRESS AS A FUNCTION OF TEMPERATURE AND STRAIN RATE FOR TENSILE DATA (CHURCHMAN, 24)

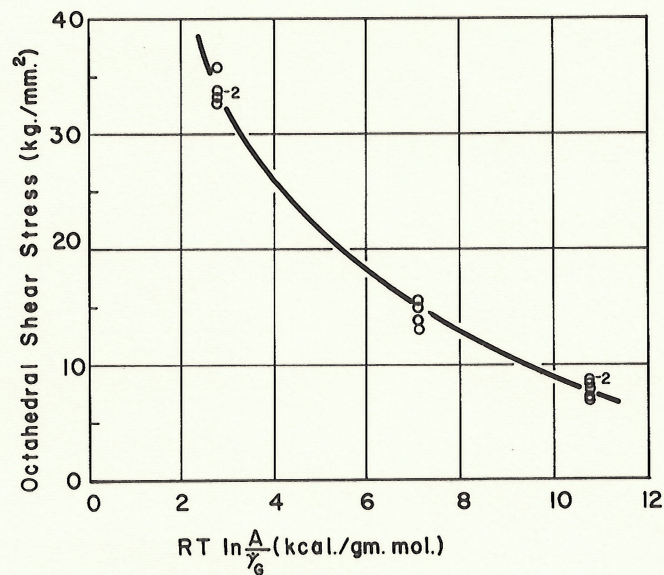


FIG.5j PROPORTIONAL LIMIT YIELD STRESS AS A FUNCTION OF TEMPERATURE AND STRAIN RATE FOR TENSILE DATA (A.A. JOHNSON, 25)

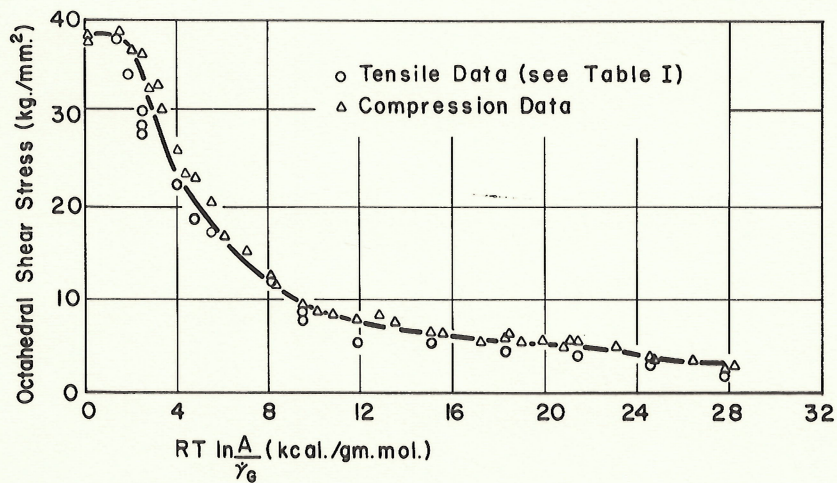


FIG.5k 0.01% OFFSET AND 0.05% OFFSET YIELD STRESS AS A FUNCTION OF TEMPERATURE AND STRAIN RATE FOR TENSILE AND COMPRESSION DATA, RESPECTIVELY (WESSEL, FRANCE AND BEGLEY, 26)

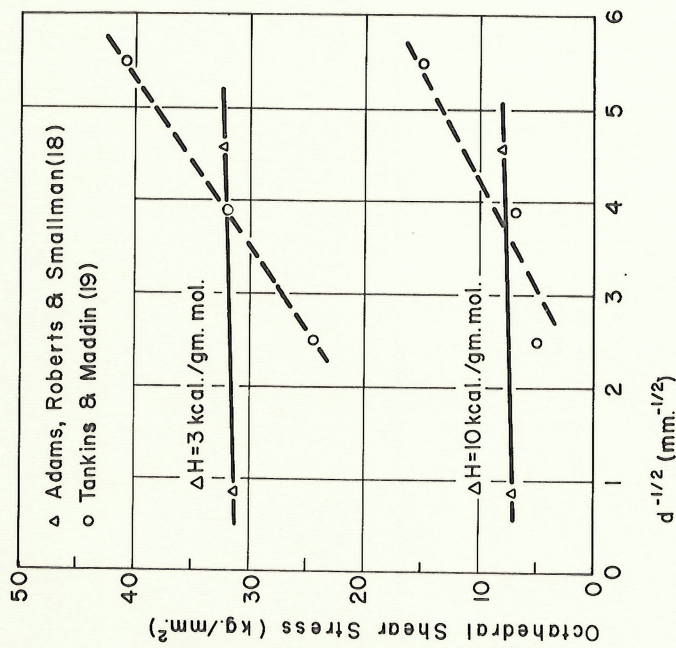


FIG.6 DEPENDENCE OF UPPER YIELD STRESS ON GRAIN DIAMETER

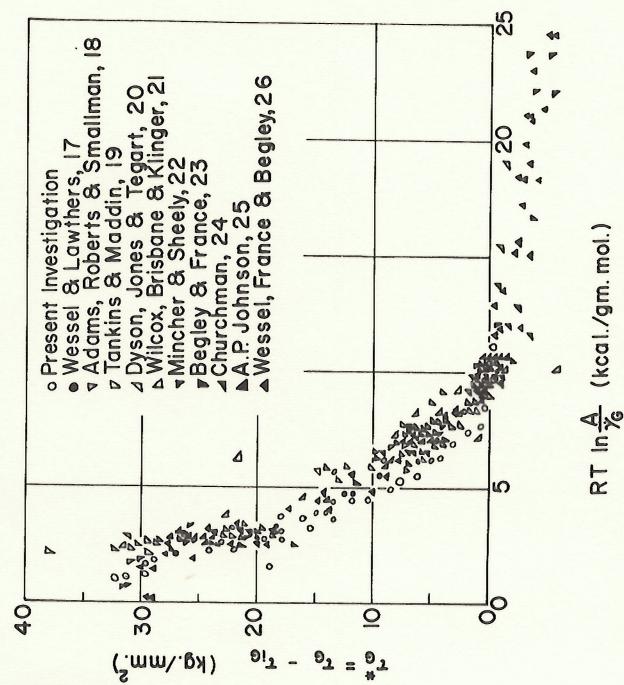


FIG.7 PARAMETER REPRESENTATION OF THE TEMPERATURE AND RATE SENSITIVE COMPONENT OF YIELD STRESS FOR NIOBIUM